No. 617 **November 2019**

The "Tensor Diffusion" approach for simulating viscoelastic fluids

P. Westervoß, S. Turek,
H. Damanik, A. Ouazzi

ISSN: 2190-1767

THE "TENSOR DIFFUSION" APPROACH FOR SIMULATING VISCOELASTIC FLUIDS

PATRICK WESTERVOSS AND STEFAN TUREK AND HOGENRICH DAMANIK AND ABDERRAHIM OUAZZI

Institute for Applied Mathematics (LS III), TU Dortmund University, Vogelpothsweg 87, 44227 Dortmund, Germany

Abstract. In this work, the novel "Tensor Diffusion" approach for simulating viscoelastic fluids is proposed, which is based on the idea, that the extra-stress tensor in the momentum equation of the flow model is replaced by a product of the strain-rate tensor and a tensor-valued viscosity. At least for simple flows, this approach offers the possibility to reduce the full nonlinear viscoelastic model to a generalized "Tensor Stokes" problem, avoiding the need of considering a separate stress tensor in the solution process. Besides fully developed channel flows, the "Tensor Diffusion" approach is evaluated as well in the context of general two-dimensional flow configurations, which are simulated by a suitable four-field formulation of the viscoelastic model respecting the "Tensor Diffusion". However, substituting the extra-stress tensor by the "Tensor Diffusion" in the complete flow model is desired for general two-dimensional flows as well, again to be able to reduce the full nonlinear viscoelastic model to a Stokes-like problem.

1. Introduction

Numerical simulations of viscoelastic fluids are still a challenging task, especially due to the involved constitutive equations describing the complex material behaviour of the flow. Basically, for highly viscous resp. slow fluids, the flow itself may be characterized by means of the Stokes equations consisting of the conservation of mass and momentum, which read

$$\rho\frac{\partial \mathbf{u}}{\partial t} - 2\eta_s \nabla\cdot\mathbf{D}(\mathbf{u}) - \nabla\cdot\boldsymbol{\sigma} + \nabla p = \mathbf{0}, \quad \nabla\cdot\mathbf{u} = 0 \tag{1}$$

under the assumption of isothermal and incompressible flows. Here, $\mathbf{u}$ denotes the velocity field, η_s denotes the solvent viscosity, $\mathbf{D}(\mathbf{u}) = \frac{1}{2}\left(\nabla\mathbf{u} + \nabla\mathbf{u}^\top\right)$ refers to the strain-rate tensor, i.e. the symmetric part of the velocity gradient, and p to the pressure field. When predicting the material behaviour of viscoelastic fluids, the Stokes equations (1) are complemented by an additional so-called constitutive equation with respect to the extra-stress tensor $\boldsymbol{\sigma}$. For motivating the novel approach presented in this work, typical techniques for modelling viscoelastic fluids are briefly discussed in the following.

In this context, constitutive equations of differential type are quite straightforward to apply, since these equations can be treated numerically in similar manner as the Stokes equations themselves. The corresponding set of nonlinear equations consists of the Stokes equations (1) together with the differential material model

$$\frac{\partial\boldsymbol{\sigma}}{\partial t} + (\mathbf{u}\cdot\nabla)\boldsymbol{\sigma} - \nabla\mathbf{u}^\top\cdot\boldsymbol{\sigma} - \boldsymbol{\sigma}\cdot\nabla\mathbf{u} + \mathbf{f}(\Lambda,\eta_p,\boldsymbol{\sigma}) = 2\frac{\eta_p}{\Lambda}\mathbf{D}(\mathbf{u}) \tag{2}$$

E-mail address: (P. Westervoß) pwesterv@math.tu-dortmund.de.

regarding the extra-stress tensor $\boldsymbol{\sigma}$. Here, Λ denotes the (single-mode) relaxation time and η_p the "polymeric" viscosity of the fluid at hand. Commonly used models are the Oldroyd-B model (or Upper-Convected Maxwell model, UCM, [1, 2], for $\eta_s = 0$ in Eq. (1)), where

$$\mathbf{f}(\Lambda, \eta_p, \boldsymbol{\sigma}) = \frac{1}{\Lambda}\boldsymbol{\sigma} \tag{3}$$

or the Giesekus model, where

$$\mathbf{f}(\Lambda, \eta_p, \boldsymbol{\sigma}) = \frac{1}{\Lambda}\left(\boldsymbol{\sigma} + \alpha\frac{\eta_p}{\Lambda}\boldsymbol{\sigma}\cdot\boldsymbol{\sigma}\right) \tag{4}$$

which results from the Oldroyd-B model by introducing an additional quadratic stress contribution [3].

The above models are already successfully applied to simulate several types of viscoelastic fluids, from polymer solutions [4, 5] up to polymer melts [6], which are of intensified interest in industrial applications. In all these cases, the corresponding relaxation time spectrum, especially of polymer melts, easily encompasses several decades, and multiple relaxation times need to be considered to achieve a satisfactory model of the relaxation behaviour by a superposition of exponential modes [1, 7]. Consequently, the stress tensor $\boldsymbol{\sigma}$ needs to be decomposed into a sum of single stress tensors $\boldsymbol{\sigma}_k$, each satisfying an equation of the form of (2) including separate parameters $\Lambda_k, \eta_{p,k}$. This results in a significant growth of the problem size, because each stress tensor $\boldsymbol{\sigma}_k$ needs to be considered as an independent flow variable [1, 6].

At least in this regard, constitutive equations of the integral type show a clear advantage, because applying these models allows to keep the problem size fixed even if the number of relaxation modes is increased, as these just enter the memory function. Integral constitutive equations considered in numerical flow simulations are often of the so-called time-separable Rivlin-Sawyers (or Kaye-BKZ) type [1, 8], where the stress tensor is written as an infinite integral of the form

$$\boldsymbol{\sigma}(t) = \int_{-\infty}^{t} M(t-t')\left[\phi_1(I_1, I_2)\,\mathbf{B}_{t'}(t) + \phi_2(I_1, I_2)\,\mathbf{B}_{t'}(t)^{-1}\right]dt' \tag{5}$$

In the above stress integral, ϕ_1, ϕ_2 are empirical functions to model nonlinear effects depending on the two non-trivial invariants I_1, I_2 of the Finger tensor $\mathbf{B}$, where $I_1 = \mathrm{tr}(\mathbf{B})$ and $I_2 = \frac{1}{2}\left(\mathrm{tr}(\mathbf{B})^2 - \mathrm{tr}(\mathbf{B}^2)\right)$. In contrast to differential models, considering multiple modes just affects the memory function M, which is in this context taken to be a superposition of exponentials, in detail $M(s) = \sum_{k=1}^{K} \eta_{p,k}/\Lambda_k^2 \exp(-s/\Lambda_k)$ (see [1].

In [8], several techniques for incorporating integral constitutive equations into a Finite Element framework are discussed, but most of them – like the so-called "streamline Finite Element method" or a decoupled Eulerian-Lagrangian approach – include a Lagrangian reference frame. Since in the context of the Finite Element method, the Stokes equations are considered in an Eulerian frame of reference, a corresponding approach is desired for integral constitutive equations as well. One of the most suitable approaches to handle integral material models in an Eulerian frame is the so-called "Deformation Fields Method" (DFM, [8, 9, 10, 11, 12]). A central object in this Eulerian scheme is the Finger tensor, which is evolved in time according to the differential equation

$$\frac{\partial}{\partial s}\mathbf{B}_{t'}(s) + (\mathbf{u}(s)\cdot\nabla)\,\mathbf{B}_{t'}(s) - \nabla\mathbf{u}(s)^{\top}\cdot\mathbf{B}_{t'}(s) - \mathbf{B}_{t'}(s)\cdot\nabla\mathbf{u}(s) = \mathbf{0} \tag{6}$$

in $s \in [t', t]$ for fixed t', where $\mathbf{B}_{t'}(t') = \mathbf{I}$.

Obviously, both kinds of modelling approaches, i.e. the differential as well as the integral material model, (2) or (5), give rise to numerical challenges due to the complex rheology of the considered viscoelastic fluids. On the one hand, in the differential case, the well-known "High Weissenberg Number Problem" (HWNP, [4, 5]) together with the need of considering multiple modes [6] need to be covered. On the other hand, for integral consitutive equations, a suitable numerical treatment of the resulting integro-differential set of equations needs to be derived [8, 9, 10, 11, 12].

Therefore, in this work, the novel "Tensor Diffusion" approach, offering the possibility to remove the complex rheology of the fluid from the set of equations and to establish a straightforward numerical treatment of viscoelastic fluids, is introduced in Sec. 2. In Sec. 3, the "Tensor Diffusion" approach is validated for quite simple flow configurations like fully developed channel flows, followed by a narrow evaluation in the context of more complex flows, i.e. the "Flow around cylinder" benchmark, in Sec. 4.

2. The "Tensor Diffusion" approach

As outlined above, many difficulties and challenges in simulating viscoelastic fluids arise from the complex rheology of the fluid characterized by both, differential and integral constitutive equations. Consequently, avoiding the need of considering such an equation at all would probably improve the general numerical treatment of such fluids. Thus, the underlying assumption of the novel "Tensor Diffusion" approach is the existence of a decomposition of the extra-stress tensor according to

$$\boldsymbol{\sigma} = \boldsymbol{\mu} \cdot \mathbf{D}(\mathbf{u}) \tag{7}$$

where $\boldsymbol{\mu} \in \mathbb{R}^{2\times 2}$ or $\boldsymbol{\mu} \in \mathbb{R}^{3\times 3}$, both for two-dimensional configurations. Inserting the stress decomposition (7) into the steady-state version of the Stokes equations (1) gives the so-called "Tensor Stokes" problem

$$-\nabla \cdot (\boldsymbol{\mu} \cdot \mathbf{D}(\mathbf{u})) + \nabla p = \mathbf{0}, \qquad \nabla \cdot \mathbf{u} = 0 \tag{8}$$

When assuming that the so-called "Tensor Diffusion" $\boldsymbol{\mu}$ from Eq. (7) or (8) is known or given corresponding to an actual viscoelastic flow problem, the "nonlinear" velocity and pressure solution, originally resulting from the (direct steady) nonlinear differential or integral viscoelastic model, can be computed by simply solving the "Tensor Stokes" problem (8) in $(\mathbf{u}, p)$, only. The part of the original problem causing most challenges and difficulties in the numerical simulation of viscoelastic fluids in genereal, i.e. the constitutive equation or the complex rheology of such fluids, is removed from the system, and the corresponding stresses are computed in post-processing fashion based on the velocity solution calculated from Eq. (8). Furthermore, a robust, efficient, accurate and stable numerical scheme can be used for solving the "Tensor Stokes" problem (8), since typical solution techniques for (generalized) Stokes problems are applicable in this context.

Obviously, the "Tensor Stokes" problem represents an extension of classical generalized Stokes equations involving a shear-rate dependent *scalar viscosity* (c.f. [13]), since besides the corresponding "shear thinning" effect, in principle the full viscoelastic material behaviour is covered by the *tensor-valued viscosity* $\boldsymbol{\mu}$.

Note, that the above form of the "Tensor Stokes" problem is obtained for both, $\eta_s = 0$, i.e. for pure polymer melts, as well as for $\eta_s > 0$, where the solvent contribution $2\eta_s\mathbf{I}$ can be absorbed into the "Tensor Diffusion" $\boldsymbol{\mu}$. However, simulating so-called "no

solvent" viscoelastic fluids is even harder than those with a present solvent contribution as discussed in the following.

On the one hand, concerning the discretization of the viscoelastic model, additional challenges arise for vanishing η_s, since in case of $\eta_s > 0$, besides choosing the well-known "Stokes pair" Q_2/P_1 regarding the velocity and pressure fields, approximating the stress variable in the same space as the velocity field leads to a LBB-stable discretization [5, 14]. However, in the "no solvent" case, the diffusive operator, present for $\eta_s > 0$, is removed from the momentum equation of the original viscoelastic model, which is why the stability of the Finite Element discretization is weakened and additional stabilization needs to be inserted into the system (c.f. [5, 14, 15]). However, when introducing the above proposed "Tensor Diffusion" $\boldsymbol{\mu}$ into the Stokes equations – leading to the "Tensor Stokes" problem eventually complemented by a constitutive equation of differential or integral type – a diffusive operator is re-coupled into the system. Consequently, an LBB-stable discretization is recovered for example by the approach proposed in [5].

On the other hand, problematic issues in terms of "no solvent" viscoelastic fluids also occur regarding solution techniques for the resulting discrete (nonlinear) systems. By following [5], the highly nonlinear systems obtained by discretizing the differential or integral viscoelastic model are solved via Newton's method, where the corresponding Jacobian matrix is calculated via Finite Differencing. Unfortunately, for a vanishing solvent contribution, a Stokes-like problem of the form

$$\begin{pmatrix} 0 & \mathcal{B} \\ \mathcal{B}^\top & 0 \end{pmatrix} \begin{pmatrix} \mathbf{u} \\ p \end{pmatrix} = \begin{pmatrix} \mathbf{r_u} \\ \mathbf{r}_p \end{pmatrix} \tag{9}$$

has to be solved coupled with a discrete version of the differential or integral constitutive equation. Consequently, for both, a monolithic or decoupled solution approach, no meaningful $(\mathbf{u}, p)$- or even $\boldsymbol{\sigma}$-solution will be computable based on the Stokes-like problem in Eq. (9). In contrast, when a similar discrete system is derived based on the "Tensor Stokes" problem (8), a Stokes-like problem of the form

$$\begin{pmatrix} -\mathcal{T} & \mathcal{B} \\ \mathcal{B}^\top & 0 \end{pmatrix} \begin{pmatrix} \mathbf{u} \\ p \end{pmatrix} = \begin{pmatrix} \mathbf{r_u} \\ \mathbf{r}_p \end{pmatrix} \tag{10}$$

is obtained, where a diffusive operator is present in the upper-left block. Thus, at least conceptually, a reasonable approach is provided for calculating a $(\mathbf{u}, p, \boldsymbol{\sigma})$-solution from Eq. (10) combined with a constitutive equation for determining the stress, which is solved monolithically or in a decoupled manner, e.g. via Operator Splitting.

Furthermore, when solving the nonlinear system consisting of the Stokes equations coupled with a (differential) material model via Newton's method (see [5] for details), there are problems arising in solving the resulting linear system. Obviously, when applying typical Krylov-space methods, no preconditioners are applicable involving the diagonal part of the global (Jacobian) matrix. In similar manner, applying multigrid techniques for solving these linear systems does not allow the use of diagonal smoothers. In fact, only Vanka-like smoothers are applicable, which perform preconditioning locally on each element [16, 17, 18]. But unfortunately, we observe an at least non-robust behaviour of the multigrid solver involving these kind of smoothers, which furthermore only work for a very large amount of additional stabilization, for instance "Edge-Oriented FEM"-stabilization (EOFEM,[5, 19]). Thus, the corresponding solutions do not show a physically meaningful behaviour. So far, we are only able to successfully perform numerical simulations for the "no solvent" case when applying Newton's method in combination with UMFPACK [20] for solving the arising linear systems in a discrete fashion. But naturally, this limits the

simulations to the range of small problem sizes, only. This issue might be resolved by inserting "Tensor Diffusion" into the nonlinear system of equations in the same way as it is done above in Eq. (10). Again, this gives rise to a diffusive operator in the Jacobian matrix, potentially allowing the application of diagonal preconditioning/smoothing in iterative solvers.

However, besides at least conceptually improving the numerical treatment of "no solvent" viscoelastic fluids, one of the main potential benefits of the novel "Tensor Diffusion" approach is the possibility, to express the complex rheology by a "Tensor Diffusion" $\boldsymbol{\mu}$ instead of solving a nonlinear constitutive equation. In the following section, it will be shown, that this concept works at least for more or less simple flow configurations.

3. Proof of concept

Above, the potential benefits of the "Tensor Diffusion" approach are outlined, but only based on the assumption, that a certain decomposition of the extra-stress tensor according to Eq. (7) exists in general. In the following, the validity of this assumption is investigated by checking the ability of the "Tensor Diffusion" approach to reproduce viscoelastic flow characteristics usually resulting from differential or integral material models.

Therefore, stationary flow states for both, differential as well as integral models, are considered in the following, where in case of differential models, the stationary version of the set of equations can be obtained by simply dropping all derivatives with respect to time t. The resulting set of equation reads

$$-2\eta_s \nabla \cdot \mathbf{D}(\mathbf{u}) - \nabla \cdot \boldsymbol{\sigma} + \nabla p = \mathbf{0} \tag{11a}$$

$$\nabla \cdot \mathbf{u} = 0 \tag{11b}$$

$$(\mathbf{u} \cdot \nabla)\boldsymbol{\sigma} - \nabla \mathbf{u}^{\top} \cdot \boldsymbol{\sigma} - \boldsymbol{\sigma} \cdot \nabla \mathbf{u} + \mathbf{f}(\Lambda, \eta_p, \boldsymbol{\sigma}) = 2\frac{\eta_p}{\Lambda}\mathbf{D}(\mathbf{u}) \tag{11c}$$

In case of integral models, besides the "Stokes part", also the corresponding stress integral needs to be transformed. In the time-dependent model, in each time step a new field $\mathbf{B}_{t'}$ is created and evolved in time depending on the time-dependent velocity field $\mathbf{u}(s)$ [9]. Assuming a steady-state solution, the velocity field stays the same for all times s in the evolution equation (6), which is why only one single deformation field $\mathbf{B}$ needs to be evolved over the infinite time interval $s \in [0, \infty[$ with initial condition $\mathbf{B}(0) = \mathbf{I}$. Unfortunately, there is no steady-state solution regarding the deformation field $\mathbf{B}(s)$, but nevertheless, the stress integral will reach a stationary state due to the exponentially decaying memory function.

When transforming the stress integral to the time variable $s \in [0, \infty[$, the steady-state formulation regarding $(\mathbf{u}, p, \boldsymbol{\sigma})$ of the integral model is obtained, where the stress integral becomes

$$\boldsymbol{\sigma} = \int_0^{\infty} M(s) \left[\phi_1(I_1, I_2)\mathbf{B}(s) + \phi_2(I_1, I_2)\mathbf{B}(s)^{-1}\right] ds \tag{12}$$

complemented as before by an evolution equation for the Finger tensor $\mathbf{B}$, but for a velocity field independent of s, hence

$$\frac{\partial}{\partial s}\mathbf{B}(s) + (\mathbf{u} \cdot \nabla)\mathbf{B}(s) - \nabla \mathbf{u}^{\top} \cdot \mathbf{B}(s) - \mathbf{B}(s) \cdot \nabla \mathbf{u} = \mathbf{0} \tag{13}$$

In general, the presented (steady-state) flow models regarding viscoelastic fluids – the Stokes equations plus a differential or integral constitutive equation – hold for three-dimensional configurations. However, in this work, two-dimensional flow states are considered only, which can be recovered from differential models by assuming $\boldsymbol{\sigma} \in \mathbb{R}^{2\times 2}$. Regarding integral constitutive equations, to derive the two-dimensional formulation following [21], one has to consider the pseudo three-dimensional Finger tensor

$$\tilde{\mathbf{B}} = \begin{pmatrix} B_{11} & B_{12} & 0 \\ B_{12} & B_{22} & 0 \\ 0 & 0 & 1 \end{pmatrix}$$

Since $\det(\mathbf{B}) = 1$ holds in case of incompressible fluids, there is only one invariant of $\mathbf{B}$, i.e. $I = I_1 = I_2 = \operatorname{tr}(\mathbf{B}) + 1$ when regarding two-dimensional configurations, where $\mathbf{B} \in \mathbb{R}^{2\times 2}$ denotes the upper-left block-matrix of $\tilde{\mathbf{B}}$. This single invariant has to be inserted into the three-dimensional formulation of integral constitutive equation (12) to derive the corresponding two-dimensional version.

3.1. **Fully developed channel flows.** As a first step, fully developed channel flows for viscoelastic fluids are considered, where the corresponding configuration according to a two-dimensional flow domain is depicted in Fig. 1.

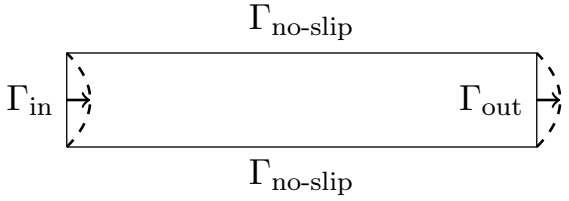

FIGURE 1. Configuration of fully developed (Poiseuille-)channel flows

In detail, for such kind of flows, the same velocity profile is obtained at any cutline over the channel height, i.e. in y-direction. Consequently, the velocity field consists only of a contribution in x-direction, i.e. the channel length, and varies only over the channel height. Similar properties hold for the stress and Finger tensors in case of differential or integral constitutive equations, respectively, which is why the flow quantities satisfy

$$\mathbf{u} = \begin{pmatrix} u \\ v \end{pmatrix} = \begin{pmatrix} u(y) \\ 0 \end{pmatrix}, \quad \frac{\partial}{\partial x}\sigma_{ij} = \frac{\partial}{\partial x}B_{ij} = 0 \tag{14}$$

where σ_{ij}, B_{ij} denote the components of $\boldsymbol{\sigma}, \mathbf{B} \in \mathbb{R}^{2\times 2}$, respectively. Applying the properties (14) to the differential steady-state version of the Upper-Convected Maxwell model, which consists of Eq. (11) together with $\eta_s = 0$ in the Stokes equations and the model function $\mathbf{f}$ from Eq. (3), leads to a linear system of equations for the unknowns $u_y, \sigma_{11}, \sigma_{12}, \sigma_{22}$. Based on the assumption, that the pressure decreases linearly in x over a channel of infinite length, i.e. $p_x \equiv \text{const} < 0$, the flow quantites can be given analytically, especially leading to the parabolic velocity profile

$$u(y) = \frac{p_x}{2\eta_p}\left(y^2 - (b+a)\,y + ba\right) \tag{15}$$

for a channel height of $y \in [a, b]$, since $u(a) = u(b) = 0$ due to $\mathbf{u} \equiv 0$ on $\Gamma_{\text{no-slip}}$ and $u_y((b+a)/2) = 0$, because of the maximum velocity being obtained on the center line of

the channel (c.f. Fig. 1). Furthermore, the corresponding (symmetric) strain-rate as well as stress tensors read

$$\boldsymbol{\sigma} = \begin{pmatrix} \sigma_{11} & \sigma_{12} \\ \sigma_{12} & \sigma_{22} \end{pmatrix} = \begin{pmatrix} 2\eta_p \Lambda u_y^2 & \eta_p u_y \\ \eta_p u_y & 0 \end{pmatrix} \tag{16a}$$

$$\mathbf{D}(\mathbf{u}) = \frac{1}{2}\begin{pmatrix} 2u_x & v_x + u_y \\ v_x + u_y & 2v_y \end{pmatrix} = \begin{pmatrix} 0 & u_y \\ u_y & 0 \end{pmatrix} \tag{16b}$$

From Eq. (16) it is realized, that indeed a matrix- or tensor-valued quantity can be derived – even analytically – relating $\boldsymbol{\sigma}$ and $\mathbf{D}$ according to Eq. (7), i.e. $\boldsymbol{\sigma} = \boldsymbol{\mu} \cdot \mathbf{D}(\mathbf{u})$, where

$$\boldsymbol{\mu} = 2\eta_p \begin{pmatrix} 1 & 2\Lambda u_y \\ 0 & 1 \end{pmatrix} \tag{17}$$

In principle, the same can be done in case of the steady-state integral version of UCM, where in a first step, the properties listed in Eq. (14) are applied to the evolution equation (13) of the Finger tensor $\mathbf{B}$, giving

$$\frac{\partial}{\partial s} B_{11}(s) = 2B_{12}(s)\, u_y, \quad \frac{\partial}{\partial s} B_{12}(s) = B_{22}(s)\, u_y, \quad \frac{\partial}{\partial s} B_{22}(s) = 0 \tag{18}$$

for $s \in [0, \infty[$. Together with the initial condition $\mathbf{B}(0) = \mathbf{I}$, the above set of equations (18) results in analytical expressions for the components of the Finger tensor, in detail

$$B_{22}(s) = 1, \quad B_{12}(s) = s u_y, \quad B_{11} = s^2 u_y^2 + 1 \quad \forall s \in [0, \infty[\tag{19}$$

Inserting Eq. (19) into the single-mode stress integral for UCM (c.f. [1]) yields

$$\begin{aligned} \boldsymbol{\sigma} &= \int_0^\infty \frac{\eta_p}{\Lambda^2} \exp\left(-\frac{s}{\Lambda}\right) (\mathbf{B}(s) - \mathbf{I})\, ds \\ &= \int_0^\infty \frac{\eta_p}{\Lambda^2} \exp\left(-\frac{s}{\Lambda}\right) \begin{pmatrix} s^2 u_y^2 & s u_y \\ s u_y & 0 \end{pmatrix} ds \\ &= \left[2\int_0^\infty \frac{\eta_p}{\Lambda^2} \exp\left(-\frac{s}{\Lambda}\right) \begin{pmatrix} s & s^2 u_y \\ 0 & s \end{pmatrix} ds\right] \left[\frac{1}{2}\begin{pmatrix} 0 & u_y \\ u_y & 0 \end{pmatrix}\right] \\ &= 2\eta_p \begin{pmatrix} 1 & 2\Lambda u_y \\ 0 & 1 \end{pmatrix} \mathbf{D}(\mathbf{u}) = \boldsymbol{\mu} \cdot \mathbf{D}(\mathbf{u}) \end{aligned} \tag{20}$$

Thus, the same stress decomposition is obtained as derived from the differential model in Eq. (16), (17). This observation is not really surprising, since the very same model is considered. But nevertheless, a stress decomposition according to $\boldsymbol{\sigma} = \boldsymbol{\mu} \cdot \mathbf{D}(\mathbf{u})$ can be derived for differential as well as integral viscoelastic models, which is a more important issue to record here.

3.1.1. *Shear flow for UCM.* For evaluating the "Tensor Diffusion" approach in terms of numerical simulations, in a first step, an even simpler flow configuration than the Poiseuille flow depicted in Fig. 1 is considered. Such a configuration is obtained by a so-called shear flow, where the velocity on the upper wall of the channel points in positive and on the lower wall in negative x-direction (c.f. Fig. 2).

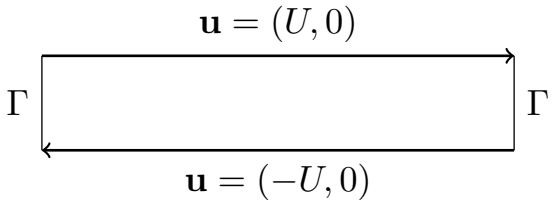

FIGURE 2. Configuration regarding shear flow

Furthermore, the resulting pressure drop in the channel vanishes and a linear velocity profile is obtained for UCM. That means, based on Eq. (16), this flow configuration results in a globally constant extra-stress as well as strain-rate tensor, consequently leading to a globally constant "Tensor Diffusion".

In the following, the velocity magnitude on the upper and lower wall of the channel is set to $U = 1.0$, from which the components of the "Tensor Diffusion" $\boldsymbol{\mu}$ can be calculated from Eq. (17), since $u_y = U$. Based on this "Tensor Diffusion", two-dimensional Finite Element simulations are performed for solving the pure "Tensor Stokes" problem (8). If the "Tensor Diffusion" approach is defined properly, the analytical linear velocity profile is recovered. Since the shear-flow configuration is quite simple, the complexity of the problem is slightly increased by setting the modified velocity profile

$$\tilde{u}(y) = Uy\left(1 + \gamma\left(1 - y^2\right)\right)$$

on the left and right edge Γ of the channel. But at the same time, the analytical "Tensor Diffusion" is prescribed globally, which is why the linear velocity profile should be recovered in the middle of the channel.

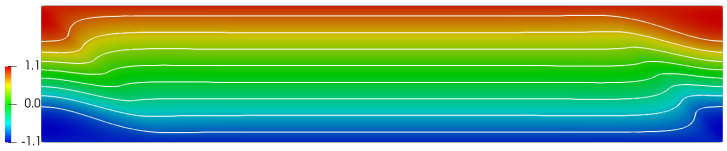

(a) x-velocity from Eq. (8), $\Lambda = 1.0$

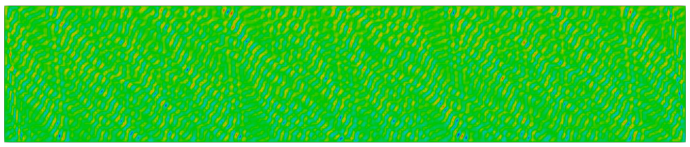

(b) x-velocity from Eq. (8), $\Lambda = 5.0$

FIGURE 3. x-velocity field for UCM, $U = 1.0, \gamma = 1.0$

For a moderate relaxation time $\Lambda = 1.0$, the resulting flow shows an appropriate behaviour. Especially, in the middle of the channel, the desired linear velocity profile is obtained, since the contour lines depicted in Fig. 3(a) are equidistant. But when Λ is increased, the flow breaks down (c.f. Fig. 3(b)) probably due to the prescribed viscosity tensor, i.e. the "Tensor Diffusion" from Eq. (17), being unsymmetric.

When instead of the original "Tensor Stokes" problem (8), a symmetrized version

$$-\frac{1}{2}\nabla \cdot \left(\boldsymbol{\mu} \cdot \mathbf{D}(\mathbf{u}) + \mathbf{D}(\mathbf{u}) \cdot \boldsymbol{\mu}^{\top}\right) + \nabla p = \mathbf{0}, \qquad \nabla \cdot \mathbf{u} = 0 \tag{21}$$

in solved, the resulting flow behaves much better (c.f. Fig. 4).

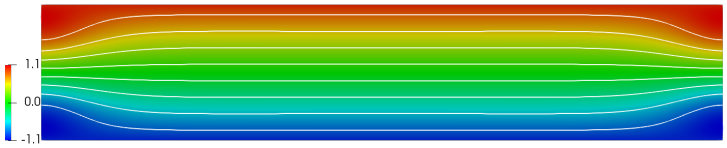

FIGURE 4. x-velocity field for UCM from Eq. (21), $\Lambda = 5.0, U = 1.0, \gamma = 1.0$

Note, that the symmetrized "Tensor Stokes" operator also satisfies the stress- decompostion (7) due to the symmetry of the extra-stress tensor, since

$$\boldsymbol{\sigma} = \frac{1}{2}\left(\boldsymbol{\sigma} + \boldsymbol{\sigma}^{\top}\right) = \frac{1}{2}\left(\boldsymbol{\mu} \cdot \mathbf{D}\left(\mathbf{u}\right) + \mathbf{D}\left(\mathbf{u}\right) \cdot \boldsymbol{\mu}^{\top}\right) \tag{22}$$

Consequently, the symmetrized version (21) of the "Tensor Stokes" problem should be solved in terms of further investigations.

3.1.2. *Poiseuille-like flow for Giesekus model.* As shown above, a tensor-valued "viscosity" relating the extra-stress $\boldsymbol{\sigma}$ to the strain-rate tensor $\mathbf{D}\left(\mathbf{u}\right)$ can be derived from at least linear differential as well as integral constitutive equations and gives meaningful results for the shear flow-configuration depicted in Fig. 2. In the following, the "Tensor Diffusion" approach is analyzed for more complex configurations by applying a similar setting as above in terms of nonlinear material models for Poiseuille-like flows.

In case of fully developed channel flows as depicted in Fig. 1, considering the Giesekus model, i.e. Eq. (11c) and (4), leads to a one-dimensional system of equations for $u_y, \sigma_{11}, \sigma_{12}, \sigma_{22}$ in a similar way as for UCM. However, since an additional quadratic stress contribution is added in the constitutive equation, solving the resulting *nonlinear* system analytically is non-trivial [22, 23]. Instead, the nonlinear system can be solved numercially more or less straightforward on a one-dimensional grid. Thus, in each grid point, the velocity and stress fields are calculated, based on which the four components of the "Tensor Diffusion" $\boldsymbol{\mu}$ are determined simply by solving Eq. (7) in each grid point.

The resulting flow profiles regarding $\mathbf{u}$ and $\boldsymbol{\sigma}$ are depicted in Fig. 5, where the shear-thinning behaviour, typically predicted by the Giesekus model [1], can be observed in the velocity profile in Fig. 5(a). In detail, the velocity shows a large gradient close to the channel wall, but a plateau-like behaviour around the center line of the channel. The flow profiles are compared for a channel height of $y \in [-1, 1]$ against the results for UCM from Eq. (15), (16), where the parameters are set such that the maximum velocity of the parabolic profile takes a value of 1.

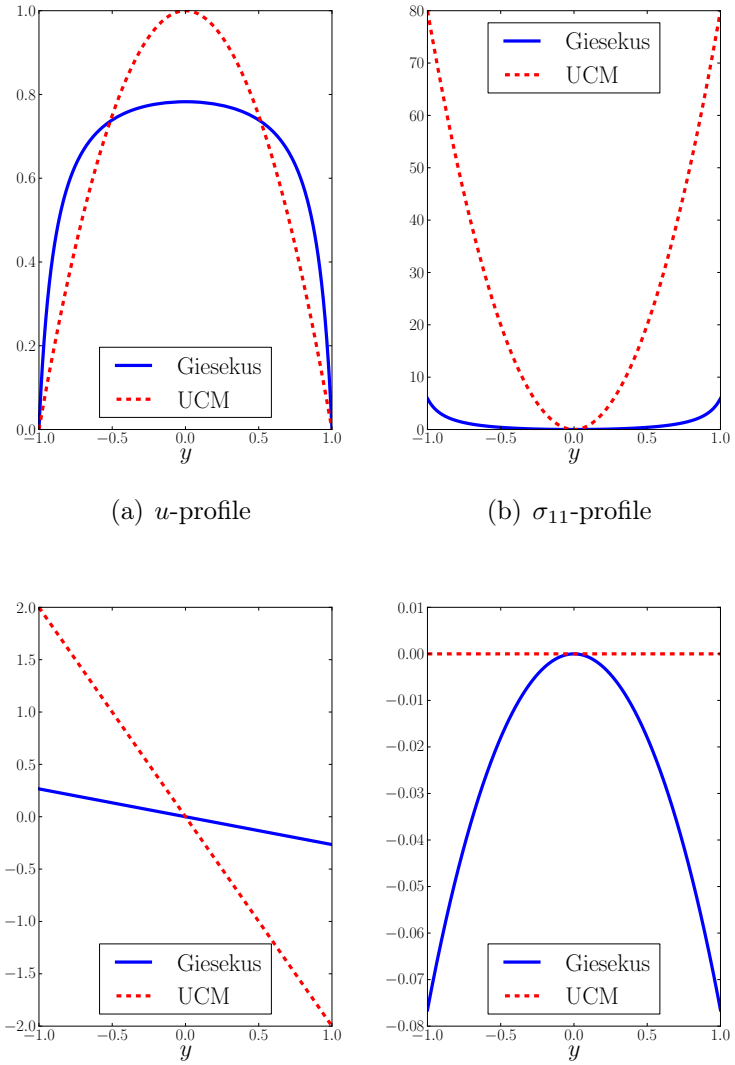

(a) u-profile (b) σ_{11}-profile

(c) σ_{12}-profile (d) σ_{22}-profile

FIGURE 5. Flow profiles for Giesekus model, $\Lambda = 10.0, \alpha = 0.1$

Based on these velocity- and stress-profiles, the corresponding profiles of the "Tensor Diffusion" $\boldsymbol{\mu}$ are calculated by solving $\boldsymbol{\sigma} = \boldsymbol{\mu} \cdot \mathbf{D}(\mathbf{u})$ for $\boldsymbol{\mu}$ in each grid point, which gives the profiles depicted in Fig. 6, where $\mu_{11} = \mu_{22}$ similar to UCM in Eq. (17).

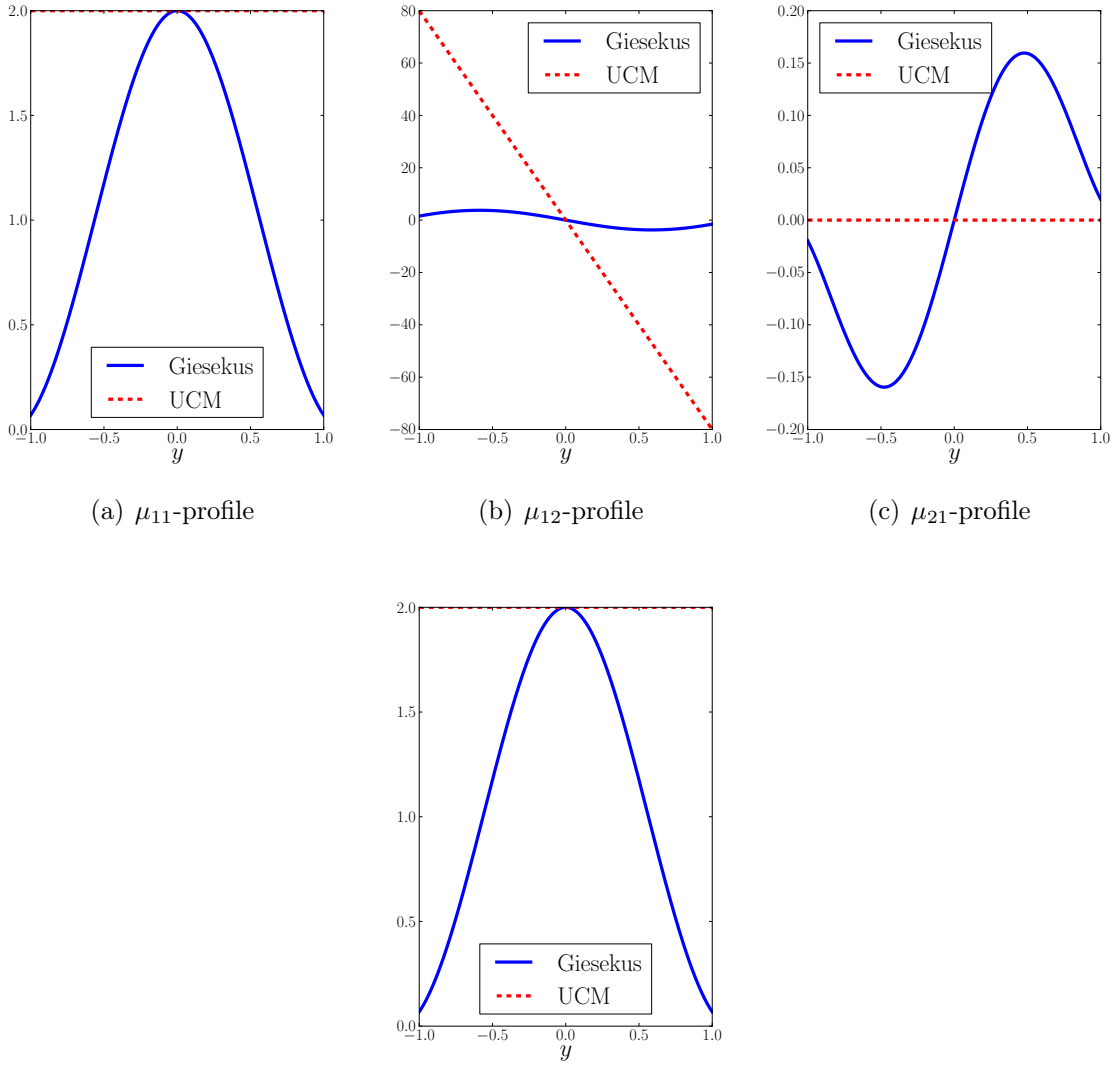

(a) μ_{11}-profile (b) μ_{12}-profile (c) μ_{21}-profile

(d) μ_{22}-profile

FIGURE 6. "Tensor Diffusion" $\boldsymbol{\mu}$ for Giesekus model, $\Lambda = 10.0, \alpha = 0.1$

Consequently, at least for the one-dimensional problem derived from the Giesekus model, a "Tensor Diffusion" can be determined, such that $\boldsymbol{\sigma} = \boldsymbol{\mu} \cdot \mathbf{D}(\mathbf{u})$.

Additionally, the "Tensor Diffusion" depicted in Fig. 6 is applied in the symmetrized "Tensor Stokes" problem (21), which is solved for a modified Poiseuille flow. In detail, a parabolic velocity profile is set as in- and outflow-profile in terms of non-homogeneous Dirichlet boundary conditions [24]. However, since the "Tensor Diffusion" $\boldsymbol{\mu}$ from Fig. 6 corresponding to the fully developed nonlinear viscoelastic flow is prescribed on every y-cutline, i.e. globally in the computational domain, the velocity profile depicted in Fig. 5(a) should be recovered away from the in- and outflow edges (c.f. Fig. 7), especially showing the expected shear-thinning effect.

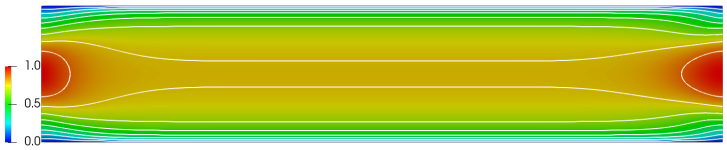

(a) x-velocity from 2D

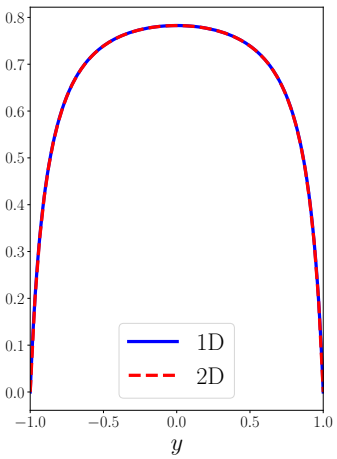

(b) x-velocity at x_{mid}

FIGURE 7. Channel flow for Giesekus model, $\Lambda = 10.0, \alpha = 0.1$

Thus, simply by solving a Stokes-like problem (21) including the newly introduced symmetrized "Tensor Diffusion", the viscoelastic flow corresponding to the nonlinear differential material model is computed.

3.1.3. *Poiseuille-like flow for PSM.* As a next step, nonlinear *integral* viscoelastic models are considered. When applying the findings based on the properties (14) to the PSM model, where the "damping function" in the stress integral (12) is chosen according to

$$\phi_1 = \frac{1}{1+\gamma\,(I-2)}, \quad \phi_2 = 0 \tag{23}$$

the stress integral becomes

$$\boldsymbol{\sigma} = \frac{\eta_p}{\Lambda^2}\int_0^\infty \exp\left(-\frac{s}{\Lambda}\right)\frac{1}{1+\gamma s^2 u_y^2}\left[\begin{pmatrix} s^2u_y^2 & su_y \\ su_y & 0\end{pmatrix} + \mathbf{I}\right] ds \tag{24}$$

The first of the two summands in the integral (24) can be treated in principle accordingly to UCM in Eq. (20), giving

$$\boldsymbol{\sigma} = \left\{2\frac{\eta_p}{\Lambda^2}\int_0^\infty \exp\left(-\frac{s}{\Lambda}\right)\frac{1}{1+\gamma s^2 u_y^2}\begin{pmatrix} s & s^2u_y \\ 0 & s\end{pmatrix} ds\right\}\mathbf{D}\,(\mathbf{u}) + \boldsymbol{\nu} \tag{25}$$

where $\boldsymbol{\nu}$ denotes a diagonal matrix. In detail, the corresponding non-zero entries consist of the infinite integral over the single-mode memory function multiplied with the damping function from Eq. (23) reading

$$\nu := \nu_{11} = \nu_{22} = \frac{\eta_p}{\Lambda^2} \int_0^\infty \exp\left(-\frac{s}{\Lambda}\right) \frac{1}{1+\gamma s^2 u_y^2} ds, \quad \nu_{12} = \nu_{21} = 0 \tag{26}$$

Thus, a "generalized" stress decomposition compared to Eq. (7) of the form

$$\boldsymbol{\sigma} = \boldsymbol{\mu} \cdot \mathbf{D}(\mathbf{u}) + \boldsymbol{\nu} \tag{27}$$

is obtained, which gives

$$\nabla p = \nabla \cdot \boldsymbol{\sigma} = \frac{1}{2} \nabla \cdot (\boldsymbol{\mu} \cdot \mathbf{D}(\mathbf{u}) + \mathbf{D}(\mathbf{u}) \cdot \boldsymbol{\mu}) + \nabla \cdot \boldsymbol{\nu} \tag{28}$$

after being inserted into the symmetrized "Tensor Stokes" problem (21). Since ν from Eq. (26) is in principle a function of u_y (and thus y itself), the additional quantity $\nabla \cdot \boldsymbol{\nu}$ in Eq. (28) can be considered as $\nabla \nu$. Consequently – even for a stress-decomposition of the type (25) – by introducing the modified pressure $P = p - \nu$, again a (symmetrized) version of the "Tensor Stokes" problem can be derived similar to Eq. (21), but now replacing the original pressure p by the modified pressure P. Thus, the "isotropic" part $\boldsymbol{\nu}$ of the stress-decomposition (25) does not affect the velocity field, but the pressure-solution only.

In contrast to the nonlinear *differential* Giesekus model, where the components of the "Tensor Diffusion" are derived numerically, in case of PSM all components of $\boldsymbol{\mu}$ as well as $\boldsymbol{\nu}$ can be explicitely written as functions of u_y. Consequently, for fully developed channel flows, the full integral viscoelastic model – including the complex rheology arising from the stress-integral over a time-interval of infinite length – is transformed into a generalized Stokes-like problem

$$-\frac{1}{2} \nabla \cdot \left(\boldsymbol{\mu}(u_y) \cdot \mathbf{D}(\mathbf{u}) + \mathbf{D}(\mathbf{u}) \cdot \boldsymbol{\mu}(u_y)^\top \right) + \nabla p = 0, \quad \nabla \cdot \mathbf{u} = 0 \tag{29}$$

consisting of a tensor-valued viscosity $\boldsymbol{\mu}$, where the corresponding entries are calculated based on u_y according to

$$\mu_{11} = \mu_{22} = 2\frac{\eta_p}{\Lambda^2} \int_0^\infty \exp\left(-\frac{s}{\Lambda}\right) \frac{s}{1+\gamma s^2 u_y^2} ds \tag{30a}$$

$$\mu_{12} = 2\frac{\eta_p}{\Lambda^2} \int_0^\infty \exp\left(-\frac{s}{\Lambda}\right) \frac{s^2 u_y}{1+\gamma s^2 u_y^2} ds \tag{30b}$$

$$\mu_{21} = 0 \tag{30c}$$

Note, that only $(\mathbf{u}, p)$ represent the remaining unknowns for simulating a nonlinear viscoelastic channel flow problem originally described by the PSM model. Obviously, integrals over infinite time still have to be computed due to Eq. (30), since the components of $\boldsymbol{\mu}$ are hardly given in closed form. But at least, the stress- or Finger-tensor is completely taken out of the system.

When the generalized "Tensor Stokes" problem (29) is solved again for a parabolic in- and outflow profile, where the "Tensor Diffusion" is defined according to Eq. (30) for an arbitrary choice of the material parameter $\gamma = 0.1$, similar to the Giesekus model depicted in Fig. 7, again a typical shear-thinning behaviour is observed (c.f. Fig. 8).

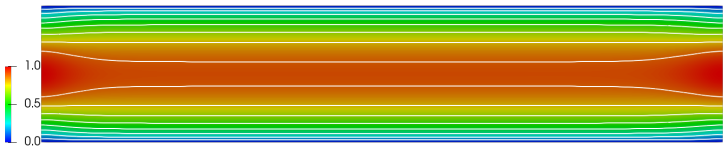

(a) x-velocity from 2D

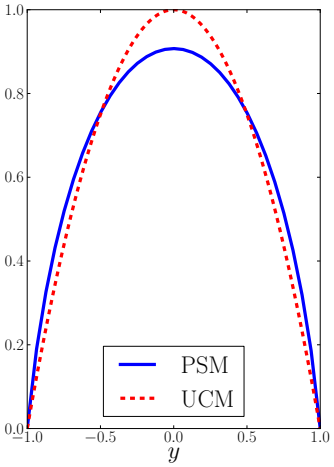

(b) x-velocity at x_{mid}

FIGURE 8. Channel flow for PSM, $\Lambda = 1.0, \gamma = 0.1$

The corresponding profiles of the "Tensor Diffusion" $\boldsymbol{\mu}$ are depicted in Fig. 9, where $\mu_{21} = 0$ in contrast to the Giesekus model (c.f. Fig. 6(c)). However, a non-vanishing behaviour of this "Tensor Diffusion" component is established, when the isotropic contribution $\boldsymbol{\nu}$ from Eq. (27) is taken into account.

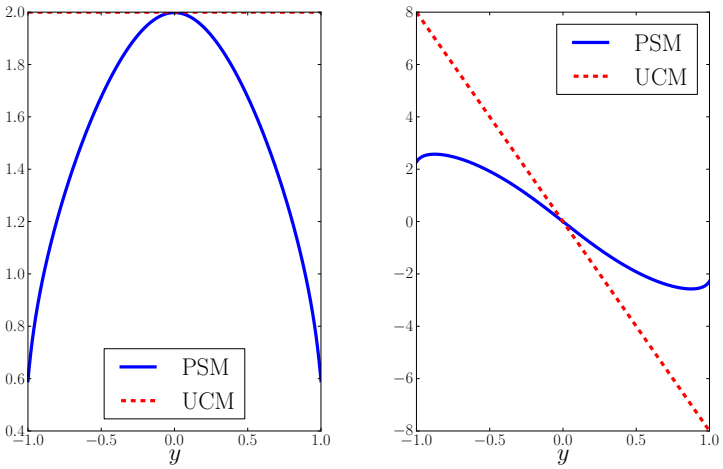

(a) μ_{11}, μ_{22}-profile (b) μ_{12}-profile

FIGURE 9. "Tensor Diffusion" $\boldsymbol{\mu}$ for PSM, $\Lambda = 1.0, \gamma = 0.1$

3.1.4. *Poiseuille-like flow for Wagner model.* However, the main drawback of the "Tensor Diffusion" approach in the context of PSM is the need to perform "infinite" integration for

computing the components of $\boldsymbol{\mu}$, which is why the numerical effort is quite high – although the original integral model is reduced to a problem in $(\mathbf{u}, p)$ only. There would be a huge improvement in the "Tensor Diffusion" approach regarding fully developed channel flows, if $\boldsymbol{\mu}$ could be modelled in terms of u_y in closed form.

Fortunately, this is the case for the Wagner model, where the damping function in the stress integral (12) is chosen as

$$\phi_1 = f \exp\left(-n_1\sqrt{I-2}\right) + (1-f)\exp\left(-n_2\sqrt{I-2}\right), \quad \phi_2 = 0 \tag{31}$$

Similar to PSM in Eq. (24), the stress integral for fully developed channel flows in case of the Wagner model results in

$$\begin{aligned}
\boldsymbol{\sigma} \;=\; & \left\{ 2\frac{\eta_p}{\Lambda^2}\int_0^\infty \left[f\exp\left(-s\left(\frac{1}{\Lambda}+n_1\sqrt{u_y^2}\right)\right) + \dots \right.\right. \\
& \left.\left. (1-f)\exp\left(-s\left(\frac{1}{\Lambda}+n_2\sqrt{u_y^2}\right)\right)\right] \begin{pmatrix} s & s^2u_y \\ 0 & s \end{pmatrix} ds \right\} \mathbf{D}(\mathbf{u}) \\
& + \frac{\eta_p}{\Lambda^2}\int_0^\infty f\exp\left(-s\left(\frac{1}{\Lambda}+n_1\sqrt{u_y^2}\right)\right) + \dots \\
& (1-f)\exp\left(-s\left(\frac{1}{\Lambda}+n_2\sqrt{u_y^2}\right)\right)\mathbf{I}\,ds
\end{aligned} \tag{32}$$

Consequently, a "generalized" stress decomposition similar to the PSM-case in Eq. (24) is derived, but in contrast to PSM, the components of the "Tensor Diffusion" $\boldsymbol{\mu}$ as well as the isotropic contribution $\boldsymbol{\nu}$ can be given in closed form. In detail,

$$\mu_{11} = 2\eta_p\left[\frac{f}{\left(1+n_1\Lambda\sqrt{u_y^2}\right)^2} + \frac{1-f}{\left(1+n_2\Lambda\sqrt{u_y^2}\right)^2}\right] \tag{33a}$$

$$\mu_{12} = 4\eta_p\Lambda u_y\left[\frac{f}{\left(1+n_1\Lambda\sqrt{u_y^2}\right)^3} + \frac{1-f}{\left(1+n_2\Lambda\sqrt{u_y^2}\right)^3}\right] \tag{33b}$$

$$\nu = \frac{\eta_p}{\Lambda}\left[\frac{f}{\left(1+n_1\Lambda\sqrt{u_y^2}\right)} + \frac{1-f}{\left(1+n_2\Lambda\sqrt{u_y^2}\right)}\right] \tag{33c}$$

besides $\mu_{22} = \mu_{11}$ and $\mu_{21} = 0$. Hence, the symmetrized "Tensor Stokes" problem (29) can be written as a nonlinear problem in the unknowns $(\mathbf{u}, p)$ only – without the need of computing infinite integrals as in Eq. (30), since the corresponding expressions in Eq. (32) for the Wagner model can be calculated exactly (c.f. Eq. (33)).

Note, that the prefactors of the components of the "Tensor Diffusion" given in Eq. (33) coincide with the entries of $\boldsymbol{\mu}$ obtained from UCM (c.f. Eq. (17)). Thus, the "Tensor Diffusion" regarding nonlinear integral models possibly arises from UCM by a suitable scaling with a fractional (or exponential) function, which might help to derive a closed form of the $\boldsymbol{\mu}$-components in the case of PSM.

However, having the analytical form of the "Tensor Diffusion" $\boldsymbol{\mu}$ for the Wagner model given in Eq. (33), again, the "Tensor Stokes" problem (29) – now of the type resulting from classical generalized Stokes equations involving a shear-rate dependent *scalar viscosity* (c.f. [13]) – is solved for the modified Poiseuille flow, where the velocity on in- and outflow-edges is again set to take a parabolic profile. However, since the "Tensor Diffusion", i.e. a *tensor-valued viscosity*, corresponding to a fully developed channel flow is prescribed

globally, the flow should evolve to its fully developed nonlinear shape away from the in- and outflow.

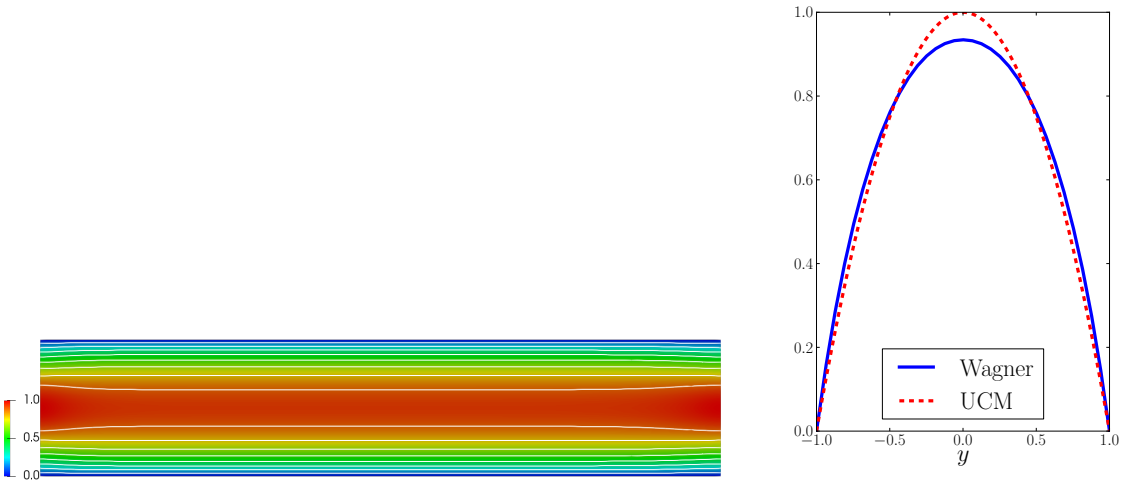

(a) x-velocity from 2D (b) x-velocity at x_{mid}

FIGURE 10. Channel flow for Wagner model, $\Lambda = 1.0, f = 0.57, n_1 = 0.31, n_2 = 0.106$

In principle, the flow profiles obtained from the Wagner model for the material parameters given in [25] show a similar behaviour as in the PSM-case, i.e. again a shear-thinning behaviour is observed for the velocity profile depicted in Fig. 10. But obviously, the "Tensor Diffusion" $\boldsymbol{\mu}$ is not differentiable in the center line of the channel (c.f. Fig. 11(a)) resulting from the denominator of the corresponding analytical expression in Eq. (33).

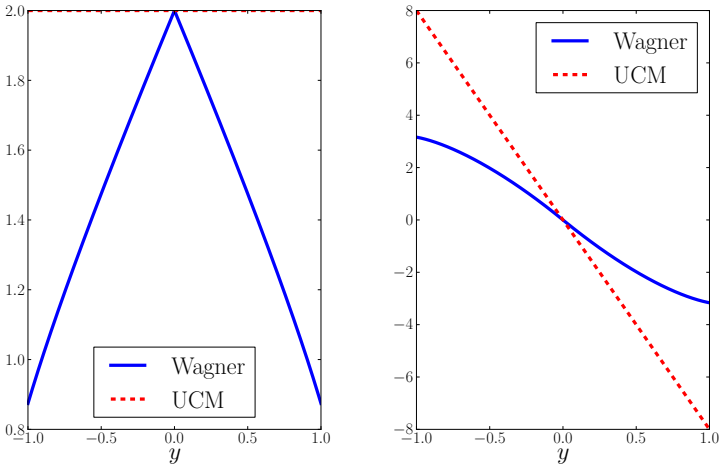

(a) μ_{11}, μ_{22}-profile (b) μ_{12}-profile

FIGURE 11. Flow profiles for Wagner model, $\Lambda = 1.0, f = 0.57, n_1 = 0.31, n_2 = 0.106$

Consequently, also for nonlinear integral models, viscoelastic flow characteristics in fully developed channel flows are reproduced by simply solving a generalized Stokes-like problem of the form (29) in the unknowns $(\mathbf{u}, p)$, where the complex rheology arising from

the stress integral is completely hidden in the "Tensor Diffusion". In case of the Wagner model, it is even possible to explicitely model the "Tensor Diffusion" depending on the "shear rate" u_y, only.

Hence, for fully developed channel flows, the overall steady-state version of the integral viscoelastic model consisting of (the stationary versions of) Eq. (1), (12), (13) can be reduced to a generalized "Tensor Stokes" problem, with explicitely given "Tensor Diffusion" $\boldsymbol{\mu}$ depending only on the shear rate of the flow. Thus, as a main result of the above investigations, especially for integral viscoelastic models, a stress-decomposition of the form $\boldsymbol{\sigma} = \boldsymbol{\mu} \cdot \mathbf{D}(\mathbf{u})$ can be given explicitely. Consequently, the "nonlinear" velocity and pressure solution, originally resulting from the nonlinear differential or integral viscoelastic model, can be computed by simply solving the symmetrized "Tensor Stokes" problem (8) in $(\mathbf{u}, p)$ only and determining the corresponding extra-stress tensor $\boldsymbol{\sigma}$ by simple postprocessing.

4. Complex flow configurations

So far, the proposed "Tensor Diffusion" approach is analyzed only in the context of fully developed channel flows due to the corresponding simple flow properties, for which it is possible, to derive and verify the validity of this novel approach. When more general two-dimensional flow configurations shall be investigated in terms of the "Tensor Diffusion" approach, an explicit derivation of the corresponding tensor-valued viscosity $\boldsymbol{\mu}$ is not (yet?) possible. Thus, this quantity might be determined numerically. A straightforward implementation for determining the "Tensor Diffusion" is obtained by complementing the original differential steady-state viscoelastic model by an additional algebraic equation regarding $\boldsymbol{\mu}$, which results in

$$-2\eta_s \mathbf{D}(\mathbf{u}) - \nabla \cdot \boldsymbol{\sigma} + \nabla p = \mathbf{0} \tag{34a}$$

$$\nabla \cdot \mathbf{u} = 0 \tag{34b}$$

$$(\mathbf{u} \cdot \nabla)\boldsymbol{\sigma} - \nabla \mathbf{u}^{\top} \cdot \boldsymbol{\sigma} - \boldsymbol{\sigma} \cdot \nabla \mathbf{u} + \mathbf{f}(\Lambda, \eta_p, \boldsymbol{\sigma}) = 2\frac{\eta_p}{\Lambda}\mathbf{D}(\mathbf{u}) \tag{34c}$$

$$\boldsymbol{\mu} \cdot \mathbf{D}(\mathbf{u}) - \boldsymbol{\sigma} = 0 \tag{34d}$$

Note, that in principle, the integral viscoelastic model can be treated in the same way.

However, in Eq. (34), the solution regarding $(\mathbf{u}, p, \boldsymbol{\sigma})$ is not affected by the "Tensor Diffusion" $\boldsymbol{\mu}$, which is computed in pure post-processing fashion, only. That changes, when similar to Eq. (8), the stress decomposition (7) is inserted into the momentum equation (34a) leading to

$$-2\eta_s \mathbf{D}(\mathbf{u}) - \frac{1}{2}\nabla \cdot \left(\boldsymbol{\mu} \cdot \mathbf{D}(\mathbf{u}) + \mathbf{D}(\mathbf{u}) \cdot \boldsymbol{\mu}^{\top}\right) + \nabla p = \mathbf{0} \tag{35a}$$

$$\nabla \cdot \mathbf{u} = 0 \tag{35b}$$

$$(\mathbf{u} \cdot \nabla)\boldsymbol{\sigma} - \nabla \mathbf{u}^{\top} \cdot \boldsymbol{\sigma} - \boldsymbol{\sigma} \cdot \nabla \mathbf{u} + \mathbf{f}(\Lambda, \eta_p, \boldsymbol{\sigma}) = 2\frac{\eta_p}{\Lambda}\mathbf{D}(\mathbf{u}) \tag{35c}$$

$$\boldsymbol{\mu} \cdot \mathbf{D}(\mathbf{u}) - \boldsymbol{\sigma} = 0 \tag{35d}$$

Now, in this four-field formulation (35) of the "Tensor Stokes" problem, the solution regarding velocity, pressure and stress is coupled with the "Tensor Diffusion" $\boldsymbol{\mu}$. In principle, this problem formulation is similar to the "Discrete Elastic Viscous Stress Splitting" (DEVSS, [26, 27, 28]), since the problem size is increased accordingly by introducing an additional variable in terms of a diffusive contribution. But in contrast to DEVSS, diffusion is introduced here in a much more natural way corresponding to the characteristic of

the actual flow, since it is linked in a meaningful way to the stress tensor itself – instead of a Newtonian-like quantity introduced in DEVSS.

In the following, the four-field formulation of the "Tensor Stokes" problem presented in Eq. (35) is analyzed regarding more complex configurations than the channel flows discussed in Sec. 3. Therefore, the "Tensor Diffusion" $\boldsymbol{\mu}$ is discretized within the Finite Element framework presented in [5] by seeking corresponding approximations in

$$\begin{aligned} \boldsymbol{M}_h &= \left\{ \mathbf{m}_h \in \left(L^2\left(\Omega_h\right)\right)^4 \mid \mathbf{m}_{h|_T} \in \left(Q_0\left(T\right)\right)^4 \ \forall T \in \mathcal{T}_h \right\} \\ Q_0\left(\hat{T}\right) &= \left\{ q \circ \Phi_{\hat{T}}^{-1} \mid q \in \langle 1 \rangle \right\} \end{aligned}$$

where Q_0 defines the space of constant functions on the reference element $\hat{T}$. Similar to the numerical treatment of the differential viscoelastic model discussed in [5], also the extended discrete nonlinear systems resulting from Eq. (34) or (35), are solved by means of a monolithic Newton-Multigrid-scheme.

However, to evaluate the principle applicability of the "Tensor Diffusion" approach in the context of general two-dimensional flow configurations, the well-known "Flow around cylinder" benchmark [5, 29, 4] is simulated by means of the four-field formulation of differential viscoelastic models including the "Tensor Diffusion" $\boldsymbol{\mu}$, both for the original model (34) as well as the "Tensor Stokes" problem (35).

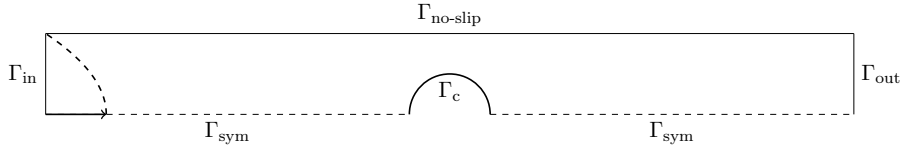

FIGURE 12. Configuration for "Flow around cylinder" benchmark

The corresponding flow configuration is depicted in Fig. 12, where the considered computational domain is of length $L = 40$ and height $H = 2$ with a confined cylinder of radius $R = 1$. On Γ_{in} and Γ_{out}, a fully developed velocity profile giving a mean velocity of $U_{\text{mean}} = 1.0$ is prescribed, where the corresponding parabolic profile reads

$$\mathbf{u} = \begin{pmatrix} u \\ v \end{pmatrix} = \begin{pmatrix} u\left(y\right) \\ 0 \end{pmatrix} = \begin{pmatrix} \frac{3}{2}\left(1 - \frac{y^2}{4}\right) \\ 0 \end{pmatrix}$$

Accordingly, the resulting stress profiles are prescribed on Γ_{in}. On the remaining boundaries, $\mathbf{u} \equiv 0$ is set on $\Gamma_{\text{no-slip}}$ and Γ_{c}, while the extra-stress is treated according to the (natural) "Do Nothing" boundary condition [24], which is furthermore applied to $\mathbf{u}$ as well as $\boldsymbol{\sigma}$ on Γ_{sym}.

As usual, the drag coefficients $C_D\left(\mathbf{T}\right)$, which are computed based on the total stress tensor $\mathbf{T}$ according to

$$C_D\left(\mathbf{T}\right) = \frac{2}{U_{\text{mean}}^2 R} F_D\left(\mathbf{T}\right), \quad F_D\left(\mathbf{T}\right) = \int_{E_{\text{c}}} \left(T_{11} n_1 + T_{xy} n_2\right) \frac{\partial \varphi}{\partial x} dx \tag{36}$$

are analyzed for evaluating the quality of the simulation results. Here, E_{c} denotes elements next to the cylinder surface Γ_{c}, n_1, n_2 denote the components of the corresponding local normal vector and φ represents a test function with support on Γ_{c}. Since in fact two problem formulations are considered, the total stress tensor for computing the drag coefficient from Eq. (36) is problem-dependent. In the following, $\mathbf{T}_\sigma$ denotes the total stress

tensor arising from the "original" viscoelastic model (34) and $\mathbf{T}_\mu$ the one corresponding to the (symmetrized) "Tensor Stokes" problem (35). Thus

$$\begin{aligned} \mathbf{T}_\sigma &= -p\mathbf{I} + 2\eta_s \mathbf{D}(\mathbf{u}) + \boldsymbol{\sigma}, \\ \mathbf{T}_\mu &= -p\mathbf{I} + 2\eta_s \mathbf{D}(\mathbf{u}) + \frac{1}{2}\left(\boldsymbol{\mu}\cdot\mathbf{D}(\mathbf{u}) + \mathbf{D}(\mathbf{u})\cdot\boldsymbol{\mu}^\top\right) \end{aligned}$$

where in principle $\boldsymbol{\sigma}$ is replaced by the symmetrized stress-decomposition to obtain $\mathbf{T}_\mu$ from $\mathbf{T}_\sigma$.

In the following, the drag coefficients for several Weissenberg numbers $\mathrm{We} = \Lambda U_{\mathrm{mean}}/R = \Lambda$ calculated via $\mathbf{T}_\mu$ are compared to reference results as well as results based on $\mathbf{T}_\sigma$, i.e. resulting from the original approach validated in [5].

In a first step, the typical benchmark configuration regarding the Oldroyd-B model is considered, i.e. Eq. (34) and (35) together with Eq. (3) are solved for a total viscosity of $\eta_0 = \eta_s + \eta_p = 1.0$ and an amount $\beta = \eta_s/\eta_0 = 0.59$ of solvent contribution. The statistics regarding the coarse mesh used for the presented simulation results are listed in Tab. 1.

level	0	1	2	3	4	5
elements	8	32	128	512	2048	8192
nodes	18	51	165	585	2193	8481
edges	25	82	292	1096	4240	16672

TABLE 1. Coarse grid for "Flow around cylinder" benchmark

A summary of the drag coefficients resulting from the above configuration is given in Tab. 2, which illustrates, that the drag coefficients obtained from the four-field formulation (35) of the "Tensor Stokes" problem show a good agreement to the results computed by means of the original method as well as the reference results [4].

We	$C_D(\mathbf{T}_\sigma)$	$C_D(\mathbf{T}_\mu)$	Ref. [4]
0.1	130.342	130.348	130.36
0.2	126.605	126.624	126.62
0.3	123.172	123.212	123.19
0.4	120.553	120.549	120.59
0.5	118.747	118.751	118.83
0.6	117.694	117.970	117.78
0.7	117.214	117.545	117.32

TABLE 2. Drag coefficients resulting from Oldroyd-B model at level 5

The same can be observed, when the Giesekus model with a mobility factor of $\alpha = 0.1$ in Eq. (4) is considered instead of the Oldroyd-B model. The resulting drag coefficients are listed in Tab. 3, where compared to Oldroyd-B, higher Weissenberg numbers can be reached, probably due to the stabilizing character of the quadratic stress term in the constitutive equation [6].

We	$C_D(\mathbf{T}_\sigma)$	$C_D(\mathbf{T}_\mu)$	Ref. [29]
0.1	125.567	125.572	125.58
0.5	103.717	103.733	103.73
1.0	95.536	95.568	95.55
5.0	85.210	85.243	–
10.0	83.047	83.068	–

TABLE 3. Drag coefficients resulting from Giesekus model, $\alpha = 0.1$, at level 5

Apparently, reference results for the Giesekus model are available only up to We = 1.0, which is why the "Tensor Stokes" results for higher Weissenberg numbers are evaluated by a comparison with the original approach only. But similar to the results obtained for the Oldroyd-B model, also in case of the Giesekus model, a good agreement of the "Tensor Stokes" results with the reference as well as the original approach is observed.

The more challenging configuration, compared to the benchmark setting discussed above, is represented by considering the "no solvent" case for the "Flow around cylinder" configuration, where $\eta_s = 0$. Unfortunately, no reference results are available for this flow configuration, which is why – similar to the Giesekus model for higher We – the "Tensor Stokes" results are again compared only against the results of the original approach. For successfully performing simulations of the "Tensor Stokes" problem for setting $\eta_s = 0$ in the momentum equation (35a), a quite large amount of stabilization is required due to the difficulties in the context of the "no solvent" case outlined in Sec. 2.

We	α	$C_D(\mathbf{T}_\sigma)$	$C_D(\mathbf{T}_\mu)$
0.1	0.0	127.373	127.403
0.5	0.0	96.046	98.054
0.1	0.1	115.377	115.508
0.5	0.1	60.804	61.992

TABLE 4. Drag coefficients resulting from UCM ($\alpha = 0.0$) or Giesekus model at level 5

However, when analyzing the calculated drag coefficients given in Tab. 4, again the "Tensor Stokes" results show a good agreement to the results of the original problem – especially for lower We for both, the UCM as well as Giesekus model. When larger Weissenberg numbers are considered, the deviation of the "Tensor Stokes" results becomes larger, since a quite large amount of stabilization has to be applied for being able to compute the corresponding solutions. Besides, for the Giesekus model it was not possible to reach significantly larger Weissenberg numbers as in the case of UCM, like it was done for a present solvent contribution above, which again illustrates the complexity of this flow configuration. But still, the "Tensor Diffusion" approach provides reasonable results.

Additionally recall, that $\boldsymbol{\mu}$ is approximated in Q_0 only, which is of lower order than the corresponding approximation of $\boldsymbol{\sigma}$ in Q_2. Naturally, results obtained from the original problem (34) are expected to be of higher accuracy anyway. But nevertheless, applying the "Tensor Diffusion" approach gives simulation results of a similar quality as the original approach. Consequently, the novel "Tensor Diffusion" approach provides reasonable results for the "Flow around cylinder" benchmark – even for very challenging configurations like the "no solvent" case – indicating the principle applicability of this technique also in case of complex flow configurations.

5. Conclusion

In this work, the novel "Tensor Diffusion" approach is introduced, where in principle the extra-stress tensor in the momentum equation of the viscoelastic model is replaced by a product of the so-called "Tensor Diffusion" and the strain-rate tensor.

The underlying assumption, that such a stress decomposition exists in general, is verified in a first step for fully developed channel flows. In this context, the validity of the approach is analyzed by reproducing solutions originally arising from differential or integral (non)linear viscoelastic flow models. Additionally, for these simple flow configurations, the "Tensor Diffusion" can be given (semi-)analytically, offering the possibility to reduce the full viscoelastic model to a generalized "Tensor Stokes" problem, i.e. a generalized Stokes-like problem including a tensor-valued viscosity. Consequently, the nonlinear viscoelastic solution might be simply computed from a Stokes-like problem, where the velocity and pressure fields are the only unknowns and the corresponding extra-stress tensor is computed in simple postprocessing.

Furthermore, the principle applicability of the "Tensor Diffusion" approach in terms of general two-dimensional flow configurations is evaluated in the context of the "Flow around cylinder" benchmark. For the typical benchmark configuration, including a present solvent contribution, as well as the much more challenging "no solvent" case, the drag coefficients resulting from the original viscoelastic model as well as reference results – if available – are reproduced quite well for both, the Upper-Convected Maxwell and the Giesekus model.

However, in contrast to the simple fully developed channel flows, for general two-dimensional flow configurations, the "Tensor Diffusion" needs to be calculated numerically. Therefore, currently an algebraic equation is considered. Naturally, a further study on determining the "Tensor Diffusion" should be performed, e.g. by means of a partial differential equation arising from inserting the stress decomposition into the (differential) constitutive equation regarding the extra-stress tensor. Additionally, it should be investigated, whether the numerical solver – especially the linear solver within the Newton scheme – can be improved by applying multigrid. This is of intensified interest in the "no solvent" case, since in the original approach the linear systems for this case are solved via direct linear solvers.

But nevertheless, the main goal of future work regarding general two-dimensional configurations is to establish the novel "Tensor Diffusion" approach in the same way as proposed for fully developed channel flows. In detail, the corresponding flow model shall be reduced to a pure "Tensor Stokes" problem, that means to a Stokes-like problem involving a tensor-valued viscosity only depending on the shear-rate of the flow. Thus, viscoelastic material behaviour should be predicted without the need to consider a (differential or integral) constitutive equation or even a stress variable at all.

References

[1] R. G. Larson, *Constitutive Equations for Polymer Melts and Solutions*. Butterworths Series in Chemical Engineering, Butterworth-Heinemann, 1988.

[2] J. G. Oldroyd, "On the formulation of rheological equations of state," *Proceedings of the Royal Society of London. Series A, Mathematical and Physical Sciences*, vol. 200, no. 1063, pp. 523–541, 1950.

[3] H. Giesekus, "Die elastizität von flüssigkeiten," *Rheologica Acta*, vol. 5, pp. 29–35, 1966.

[4] M. A. Hulsen, R. Fattal, and R. Kupferman, "Flow of viscoelastic fluids past a cylinder at high weissenberg number: Stabilized simulations using matrix logarithms," *Journal of Non-Newtonian Fluid Mechanics*, vol. 127, no. 1, pp. 27 – 39, 2005.

[5] H. Damanik, J. Hron, A. Ouazzi, and S. Turek, "A monolithic fem approach for the log-conformation reformulation (lcr) of viscoelastic flow problems," *Journal of Non-Newtonian Fluid Mechanics*, vol. 165, no. 19, pp. 1105 – 1113, 2010.

[6] J. Kroll, S. Turek, and P. Westervoß, "Evaluation of nonlinear differential models for the simulation of polymer melts," *Kautschuk Gummi Kunststoffe*, pp. 48–52, Mar. 2017.
[7] C. W. Macosko, R. G. Larson, and K. (Firm), *Rheology : principles, measurements, and applications*. New York : VCH, 1994. Originally published as ISBN 1560815795.
[8] R. Keunings, "Finite element methods for integral viscoelastic fluids," 2003.
[9] E. Peters, M. Hulsen, and B. van den Brule, "Instationary eulerian viscoelastic flow simulations using time separable rivlin–sawyers constitutive equations," *Journal of Non-Newtonian Fluid Mechanics*, vol. 89, no. 1, pp. 209 – 228, 2000.
[10] M. Hulsen, E. Peters, and B. van den Brule, "A new approach to the deformation fields method for solving complex flows using integral constitutive equations," *Journal of Non-Newtonian Fluid Mechanics*, vol. 98, no. 2, pp. 201 – 221, 2001.
[11] P. Bollada and T. Phillips, "A modified deformation field method for integral constitutive models," *Journal of Non-Newtonian Fluid Mechanics*, vol. 163, no. 1, pp. 78 – 87, 2009.
[12] M. A. Hulsen and P. D. Anderson, "The deformation fields method revisited: Stable simulation of instationary viscoelastic fluid flow using integral models," *Journal of Non-Newtonian Fluid Mechanics*, vol. 262, pp. 68 – 78, 2018.
[13] A. Ouazzi and S. Turek, "Numerical methods and simulation techniques for flow with shear and pressure dependent viscosity," in *Numerical Mathematics and Advanced Applications* (M. Feistauer, V. Dolejsi, P. Knobloch, and K. Najzar, eds.), pp. 668–676, Springer, Aug. 2003. Enumath 2003 Prague; ISBN-Nr. 3-540-21460-7.
[14] J. Baranger and D. Sandri, "A formulation of stokes's problem and the linear elasticity equations suggested by the oldroyd model for viscoelastic flow," *ESAIM: Mathematical Modelling and Numerical Analysis - Modélisation Mathématique et Analyse Numérique*, vol. 26, no. 2, pp. 331–345, 1992.
[15] V. Girault and P.-A. Raviart, *Finite Element Methods for Navier-Stokes Equations: Theory and Algorithms*. Berlin, Heidelberg: Springer Berlin Heidelberg, 1986.
[16] H. Damanik, J. Hron, A. Ouazzi, and S. Turek, "A monolithic fem-multigrid solver for non-isothermal incompressible flow on general meshes," *Journal of Computational Physics*, vol. 228, no. 10, pp. 3869 – 3881, 2009.
[17] S. Turek, A. Ouazzi, and J. Hron, "A computational comparison of two FEM solvers for nonlinear incompressible flow," in *Challenges in Scientific Computing CISC 2002* (E. Bänsch, ed.), LNCSE, (Berlin), pp. 87–109, Springer, Jan. 2002. ISBN 3-540-40887-8.
[18] S. Vanka, "Block-implicit multigrid solution of navier-stokes equations in primitive variables," *Journal of Computational Physics*, vol. 65, no. 1, pp. 138 – 158, 1986.
[19] S. Turek and A. Ouazzi, "Unified edge–oriented stabilization of nonconforming FEM for incompressible flow problems: Numerical investigations," *Journal of Numerical Mathematics*, vol. 15, no. 4, pp. 299–322, 2007.
[20] T. A. Davis, "Algorithm 832 : Umfpack, an unsymmetric-pattern multifrontal method," *ACM Transactions on Mathematical Software*, vol. 30, no. 2, pp. 196–199, 2004.
[21] M. Tomé, J. Bertoco, C. Oishi, M. Araujo, D. Cruz, F. Pinho, and M. Vynnycky, "A finite difference technique for solving a time strain separable k-bkz constitutive equation for two-dimensional moving free surface flows," *Journal of Computational Physics*, vol. 311, pp. 114 – 141, 2016.
[22] J. Yoo and H. Choi, "On the steady simple shear flows of the one-mode giesekus fluid," *Rheologica Acta*, vol. 28, no. 1, pp. 13–24, 1989.
[23] G. Schleiniger and R. J. Weinacht, "Steady poiseuille flows for a giesekus fluid," *Journal of Non-Newtonian Fluid Mechanics*, vol. 40, no. 1, pp. 79 – 102, 1991.
[24] J. G. Heywood, R. Rannacher, and S. Turek, "Artificial boundaries and flux and pressure conditions for the incompressible navier–stokes equations," *International Journal for Numerical Methods in Fluids*, vol. 22, no. 5, pp. 325–352, 1996.
[25] H. M. Laun, "Description of the non-linear shear behaviour of a low density polyethylene melt by means of an experimentally determined strain dependent memory function," *Rheologica Acta*, vol. 17, pp. 1–15, Jan 1978.
[26] R. Guénette and M. Fortin, "A new mixed finite element method for computing viscoelastic flows," *Journal of Non-Newtonian Fluid Mechanics*, vol. 60, no. 1, pp. 27 – 52, 1995.
[27] F. P. Baaijens, S. H. Selen, H. P. Baaijens, G. W. Peters, and H. E. Meijer, "Viscoelastic flow past a confined cylinder of a low density polyethylene melt," *Journal of Non-Newtonian Fluid Mechanics*, vol. 68, no. 2, pp. 173 – 203, 1997. Papers presented at the Polymer Melt Rheology Conference.

[28] F. P. Baaijens, "An iterative solver for the devss/dg method with application to smooth and non-smooth flows of the upper convected maxwell fluid," *Journal of Non-Newtonian Fluid Mechanics*, vol. 75, no. 2, pp. 119 – 138, 1998.

[29] S. Claus and T. Phillips, "Viscoelastic flow around a confined cylinder using spectral/hp element methods," *Journal of Non-Newtonian Fluid Mechanics*, vol. 200, pp. 131 – 146, 2013. Special Issue: Advances in Numerical Methods for Non-Newtonian Flows.